NASA Contractor Report 187533
ICASE Report No. 91-24

ICASE

MACH 4 AND MACH 8 AXISYMMETRIC NOZZLES FOR A SHOCK TUNNEL

P. A. Jacobs
R. J. Stalker

Contract No. NAS1-18605
February 1991

Institute for Computer Applications in Science and Engineering
NASA Langley Research Center
Hampton, Virginia 23665-5225

Operated by the Universities Space Research Association

National Aeronautics and
Space Administration

Langley Research Center
Hampton, Virginia 23665-5225

MACH 4 AND MACH 8 AXISYMMETRIC NOZZLES FOR A SHOCK TUNNEL

P. A. Jacobs[1]
Institute for Computer Applications in Science and Engineering
NASA Langley Research Center
Hampton, VA 23665
U.S.A.

and

R. J. Stalker
Department of Mechanical Engineering
University of Queensland
St. Lucia, Qld 4067
AUSTRALIA

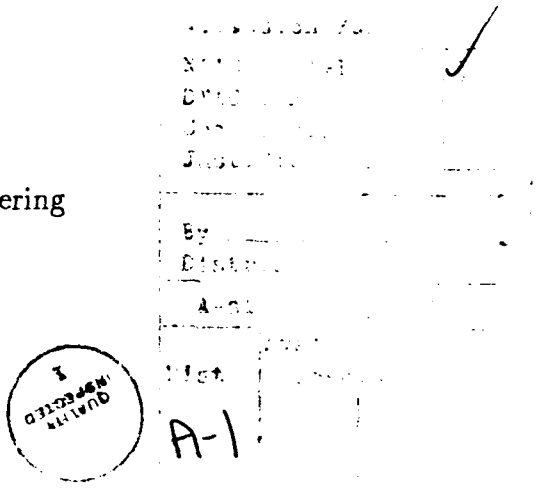

ABSTRACT

This study examines the performance of two axisymmetric nozzles which were designed to produce uniform, parallel flow with nominal Mach numbers of 4 and 8. A free-piston-driven shock tube was used to supply the nozzle with high-temperature, high-pressure test gas. The inviscid design procedure treated the nozzle expansion in two stages. Close to the nozzle throat, the nozzle wall was specified as conical and the gas flow was treated as a quasi-one-dimensional chemically-reacting flow. At the end of the conical expansion, the gas was assumed to be calorically perfect and a contoured wall was designed (using Method-of-Characteristics) to convert the source flow into a uniform and parallel flow at the end of the nozzle. Performance was assessed by measuring Pitot pressures across the exit plane of the nozzles and, over the range of operating conditions examined, the nozzles produced satisfactory test flows. However, there were flow disturbances in the Mach 8 nozzle flow that persisted for significant times after flow initiation.

[1]Research was supported at the National Aeronautics and Space Administration under NASA Contract No. NAS1-18605 while the author was in residence at the Institute for Computer Applications in Science and Engineering (ICASE), NASA Langley Research Center, Hampton, VA 23665.

Notation

a : speed of sound
d : diameter
H : total enthalpy
L : nozzle length
M : Mach number
P : pressure
r : radial coordinate
T : temperature
t : time
u : axial velocity
x : axial coordinate

γ : ratio of specific heats
Δt : time delay for normalizing
δ : boundary layer thickness
δ^* : boundary layer displacement thickness
λ : volumetric compression ratio for the driver tube
ρ : density

Subscripts:
$*$: throat condition
A, B, C, D : locations in the inviscid design
d : inviscid design value
s : nozzle supply/stagnation condition
t : truncated nozzle value

1 INTRODUCTION

In recent years there has been a renewal of interest in pulse-type aerodynamic test facilities as a way of providing experimental data for flight Mach numbers greater than 8. In particular, the free-piston-driven reflected-shock tunnel has emerged as a versatile facility covering the hypervelocity range $10 < M_{flight} < 25$ with sufficient test section density to be useful in combustion studies. See Stalker [1] and Hornung [2] for reviews of pulse facilities and their use in experimental hypervelocity aerodynamics.

When designing experiments for these facilities, the duration of the quasi-steady test flow is often a limiting factor. Typical test times range from $\frac{1}{10}$ to 3 millseconds. From the experimenter's point of view, the model size must be restricted so that the important flow features are allowed to reach steady state in the available test time (see e.g. [3]). From the facility designer's point of view, it is important to make the steady flow duration as long as

possible. Therefore, the facility nozzle must not only provide uniform and parallel flow to the test region, it should also start quickly and reach steady state while consuming as little test gas as possible. These constraints become more severe at the higher enthalpies where the facility supplies a smaller amount of test gas for a shorter time.

The approach to steady state flow in the nozzle can be influenced by unsteady processes in both the inviscid core flow, and the nozzle wall boundary layer. The inviscid wave processes cause large changes in the test flow parameters but, provided that the initial density of the gas in the nozzle is low enough, these processes tend to be completed in a time which is only a little more than the time required for the steady flow to traverse one nozzle length. The effect of the boundary layer on the test flow parameters is not always large enough to be significant but, when it is, the fact that some three flow lengths are required to produce a steady boundary layer [4] implies that viscous effects may be the cause of much longer delays in attaining steady flow in the test region.

This paper provides an overview of the design and performance of two of the contoured nozzles used on the T4 shock tunnel facility [5] located at the University of Queensland. One was designed for a nominal Mach number of 4 and, as manufactured, was $0.512m$ long with a $25.0mm$ throat diameter and a $135mm$ exit diameter. It was not expected to show significant boundary layer effects. The other nozzle, designed for a Mach number of 8, was $1.86m$ long, had a $15.24mm$ diameter throat and a $388mm$ diameter exit. Because of its greater length and higher Mach number, it was expected to be much more prone to boundary layer effects. Further details, including detail drawings of the nozzle components, may be found in [6] and [7].

In Section 2 the operation of the shock tunnel is described and the transient nature of the flow is noted. Section 3 describes the design procedure used for both nozzles. The nozzles, intended to supply test gas to model scramjet combustors, were designed using the simple flow decoupling approach described in [8]. This procedure is essentially the classical procedure as described in many text books (see e.g. [9], [10]) except for the analysis of the flow near the nozzle throat.

Both nozzles were calibrated by measuring Pitot pressures near the exit plane for a number of operating conditions. A subset of the measurements is presented in Section 4. Quasi-steady performance for both nozzles was adequate but, for the Mach 8 nozzle, it was found that the flow was taking much longer to reach steady state than initially expected. This delay in starting was the subject of numerical study [11].

2 REFLECTED-SHOCK TUNNEL OPERATION

The principal features of a free-piston driven shock tunnel, along with an approximate wave diagram, are shown in Fig. 1. The driver tube, which initially contains low pressure helium downstream of the piston, and the shock tube which contains the test gas, are separated by the primary diaphragm. This diaphragm was typically composed of two sheets of mild steel. Attached to the downstream end of the shock tube is the facility nozzle whose throat is significantly smaller than the inside diameter of the shock tube. The subsonic portion of the nozzle effectively closes the downstream end of the shock tube and forms the shock reflection region. The supersonic portion of the nozzle empties directly into a test section and dump tank which is evacuated to an initial pressure of approximately 30 Pa. The test gas is retained in the shock tube by a thin mylar diaphragm.

The first stage of operation consists of the launch of the piston and its acceleration along the compression tube. The driving force is supplied by compressed air from a reservoir. The helium in front of the piston is compressed and eventually bursts the primary diaphragm (at a pressure $56.6MPa$ for a $4mm$ thick diaphragm). After diaphragm rupture, the helium expands into the shock tube and shock-compresses the test gas before it. The *primary* shock wave travels the length of the shock tube, reflects from the closed end, and brings the test gas to rest in the nozzle supply region. Operation in this manner is called *tailored* and is shown in the wave diagram (Fig. 1(b)) by the contact surface coming to rest when intercepted by the reflected shock. Ideally the nozzle supply conditions, characterized by the total enthalpy H_s and pressure P_s, are maintained as the reflected shock continues upstream though the driver gas. In an effort to delay the arrival of the driver gas at the nozzle throat and increase the available test time, the shock tube was operated in an *undertailored* mode where the reflected shock accelerates into the driver gas and an expansion propagates into the nozzle supply region. This increases the distance between the driver-gas/test-gas interface and the end wall of the shock tube but also results in an unavoidable drop in P_s shortly after shock reflection. The net result is a typical nozzle supply pressure history as shown in Fig. 2. The transducer used to obtain this trace was located approximately $8cm$ upstream of the closed end of the shock tube. Hence, the passage of the primary and reflected shocks are shown as distinct events. Because of the location and limited response time for the transducer, the peak reflection pressure was not recorded. Once past the maximum value, P_s continued to decay due to the combined effects of undertailored operation and driver dynamics. For pure helium driver gas and operation considered here, this decay was typically $25 - 30\%$ during a nominal $0.5ms$ test time.

Upon shock reflection, the light secondary diaphragm bursts and some of the test gas

following the primary shock expands through the nozzle throat into the divergent part of the nozzle. From the point of view of the nozzle, the shock tube is now a reservoir of stagnant, high-temperature, high-pressure test gas. The subsequent starting of the nozzle has been examined experimentally and analytically by Amann [12] and Smith [13]. Note that while the Mach 4 nozzle is relatively short and is expected to start quickly, the Mach 8 nozzle is large enough for the starting time to significantly reduce the available test time. Thus a quanitative understanding of the starting processes is important.

As the primary shock travels down the nozzle it accelerates the very low pressure gas already in the nozzle. However, the primary shock decelerates because of the diverging nozzle walls. Figure 3, based on the quasi-one-dimensional model in [13] illustrates this situation. Test gas which accelerates through the nozzle throat following the primary shock, expands to a very high Mach number and is suddenly decelerated when it encounters the slower primary shock structure. An upstream-facing shock is thus formed and is swept downstream through the nozzle. Between the upstream-facing shock and the steady expansion being established near the throat there is an unsteady expansion, the upstream head of which is being swept downstream with velocity $u - a$. When the unsteady expansion is the last wave to be expelled, the starting time for the nozzle can be approximated from the steady state conditions. For higher initial pressures in the nozzle/test-section, the transit time for the upstream-facing shock will determine the nozzle starting time [13]. In the conical and wedge-shaped nozzles studied by Smith, the initial pressure could be significantly higher than the steady-state static pressure without prolonging the starting processes. However, for the Mach 8 contoured nozzle studied here, an initial pressure of a tenth of the steady-state static pressure is sufficient to delay the quasi-one-dimensional starting process [11]. A similar effect was also observed by Gregorenko *et al* [14] for high Mach number conical nozzles.

The quasi-one-dimensional model has been considered adequate for most practical situations where the divergence angle of the nozzle is small and the design Mach number of the nozzle is not too large. Britan and Vasil'ev [15], have studied two-dimensional situations in which the nozzle divergence angle is large and where multidimensional effects upstream of the throat result in high peak properties at the throat (on a time scale much smaller that the nominal test time). The numerical study in [11] did not consider such effects in the subsonic part of the nozzle but concluded that they should be included in future studies.

3 NOZZLE DESIGN

Once the test gas is brought to rest at the end of the shock tube, it is expanded to the test section conditions in two *conceptually* separate stages. First, the gas is expanded through a conical section to produce a uniform *source* flow, and then it is straightened by the contoured section of the nozzle wall so that the flow into the test section is approximately uniform and parallel. This procedure was first used to design nozzles for reflected-shock tunnels by Stalker and Daffy (circa 1972, unpublished) and is still the method of choice for high enthalpy facilities [16] where chemical reaction greatly complicates the flow analysis near the throat.

For typical facility operating conditions in the ranges $10MJ/kg < H_s < 40MJ/kg$, $10MPa < P_s < 80MPa$, chemical nonequilibrium effects have a significant effect on the nozzle flow. For example, recombination near the nozzle throat tends to keep the gas temperature high and thus produce a test flow with lower Mach number than would occur for a nonreacting flow. Thus, shock tunnel nozzles generally have larger area ratios than their perfect gas ($\gamma = 1.4$) counterparts. Also, chemical freezing can cause as much as 25% of the total enthalpy to be retained as dissociated products leaving the nozzle.

The splitting of the overall nozzle expansion into two stages allows a relatively simple analysis of the flow. A quasi-one-dimensional analysis is used in the early stages of the expansion where nonequilibrium chemical effects are important, while a standard perfect-gas method-of-characteristics analysis is used in the second stage of the expansion (i.e. the contoured wall section). Such a simplification was considered reasonable as a previous study [17] indicated that nozzle contours computed for a chemically reacting gas mixture were very similar to contours computed for a perfect gas with a suitably chosen value of γ.

3.1 Mach 4 Nozzle

The design point chosen for the Mach 4 nozzle had a nozzle supply pressure $P_s = 30.4MPa$, a supply enthalpy $H_s = 16.2MJ/kg$ and temperature $T_s = 8000K$. The throat diameter $d_* = 25.0mm$ was chosen to match that of the Mach 5 nozzle already in use on the T4 facility. A conceptual view of the entire nozzle is shown in Fig. 4. For computational convenience, we set the origin of the axial coordinate to the start of the conical expansion (immediately after the throat).

For the subsonic portion of the nozzle, most of the end of the shock-tube had been kept flat and normal to the tube axis so that the shock reflection was well behaved. The subsonic lead-in to the throat needed to be smooth in order to avoid separation and associated oblique

shocks at the beginning of the conical expansion [12]. The throat was a constant diameter section of (approximate) length d_* and was manufactured from a beryllium-copper alloy (B10 or B25). In reference [18] it was indicated that such throats produce good quality source flow when used in conical nozzles. Also, it was found that these throats resisted erosion better than those with a shorter constant-diameter section or those manufactured from grade 316 stainless steel. In operation, the Be-Cu throats of the Mach 4 nozzle did not erode noticeably.

The design of the initial conical expansion (region 2, Fig. 4) involved the analysis of the flow as a steady, quasi-one-dimensional chemically reacting flow. Flow properties were determined with the program NENZF [19] in which gas in the nozzle supply region (region 1) upstream of the throat is assumed to be stagnant and in chemical equilibrium. A chemical equilibrium model was also used in the throat but a finite-rate chemistry model was used downstream of the throat. The conical expansion had a cone half-angle of 12° and extended to $x = 0.0984m$. At this point, the reactions were assumed frozen and the gas was modelled as a perfect gas. The Mach number at the end of the conical expansion $M_A = u/a = 2.804$ where a is an estimate of the speed of sound. The value $\gamma = 1.33$ was chosen for the subsequent perfect gas calculations.

The Method-of-Characteristics (MOC) was then used to compute the source flow (region 3), the flow correcting section (region 4) and the uniform flow region (region 5) in a semi-automated way with the program described in [20]. The inlet boundary was specified as uniform source flow at 12 points along the arc AB. The Mach number on the axis at point C was computed to be $M_C = 4.12$ and, beyond this point, was held constant. The solution then stepped downstream along the axis and computed the required flow in region 4 by proceeding upstream along characteristics of the same family as CA. Once the characteristic mesh was generated, a streamline was interpolated through the mesh, starting at point A and finishing where it intersected the characteristic CD (which forms the upstream boundary of the uniform test flow region). The data points on the interpolated streamline were then fitted with a cubic-spline function [21] having eight knots and a starting slope specified to match the initial conical expansion. Table 1 displays the coordinates of the knots for the spline function.

A boundary layer correction was added to the inviscid contour as a linear variation of displacement thickness. Thus, the total wall radius was

$$r_{total} = r_{inviscid} + \frac{x}{x_D}\delta_D^* \quad , \tag{1}$$

where the boundary layer displacement thickness was estimated to be $\delta_D^* = 1.4mm$ at the nozzle exit plane [6] and $r_{inviscid}$ is given by the spline function specified in Table 1.

j	x_j (m)	r_j (m)	comment
1	0.09843	0.03343	point A, $dr/dx = 0.2126$
2	0.15748	0.04445	
3	0.21654	0.05279	
4	0.27559	0.05856	
5	0.33465	0.06230	
6	0.39370	0.06466	
7	0.45276	0.06588	
8	0.51181	0.06607	point D, natural end condition

Table 1: Knots for the cubic interpolating spline for the Mach 4 nozzle.

The fabricated nozzle is shown in cross-section in Fig. 5(A). Note that the converging (subsonic) region closes off the shock tube to form the shock reflection region. This component of the nozzle was manufactured from high-tensile steel and extended into the diverging section of the nozzle to the axial location $x = 0.15m$. The contoured wall section of the nozzle was manufactured from aluminium.

3.2 Mach 8 Nozzle

The design point chosen for the Mach 8 nozzle was the same as that for the Mach 4 nozzle (i.e. $P_s = 30.4MPa$, $H_s = 16.2MJ/kg$, $T_s = 8000K$). The throat diameter $d_* = 15.24mm$ was chosen after some iteration. The design is based on the same procedure as that used for the Mach 4 nozzle.

Again, most of the end of the shock-tube had been kept flat and normal to the tube axis so that the shock reflection was well behaved. This was not expected to cause any problem as the area ratio of the nozzle was large ($A_{exit}/A_* \simeq 667$) [22]. The throat was a constant diameter section of length d_* and was manufactured from a beryllium-copper alloy. In operation, the Be-Cu throats of the Mach 8 nozzle were observed to increase in diameter by approximately $0.5mm$ over six shots when the facility was operated at $H_s = 10MJ/kg$ and $P_s = 50 - 70MPa$.

The initial conical expansion had a cone half-angle of 14° and extended to $x = 0.168m$. At this point, the reactions were again assumed frozen and the gas was modelled as a perfect gas. The flow conditions at the end of the conical expansion were $M_A = u/a = 4.245$ and ratio of specific heats $\gamma = 1.38$. This value was chosen by considering *equivalent* chemically reacting and perfect gas flows through the same quasi-one-dimensional expansion.

j	x_j (m)	r_j (m)	comment
1	0.16800	0.04951	point A, $dr/dx = 0.2493$
2	0.45648	0.10584	
3	0.74488	0.14208	
4	1.03336	0.16552	
5	1.32176	0.18104	
6	1.61024	0.19040	
7	1.89872	0.19520	
8	2.18712	0.19688	point D, natural end condition

Table 2: Knots for the cubic interpolating spline for the Mach 8 nozzle wall.

The inlet boundary for the MOC calculation was specified as uniform source flow at 12 points along the arc AB in Fig. 4. The Mach number on the axis at point C was computed to be $M_C = 8.02$ and, beyond this point, was held constant. The solution for regions 4 and 5 was then generated and a streamline interpolated from A to D. Table 2 displays the coordinates of the knots for the spline representation of this streamline.

The design process described above produces a nozzle with the smallest inviscid design length $L_d = 2\ 187m$. However, a smoother transition may be obtained by adding a section with a smooth variation of axial Mach number between the end of the source flow region (C) and the start of the uniform test flow region. The length of the fabricated nozzle was later reduced by truncating the design contour at $L_t = 1.8m$ where the characteristic CD intersected the estimated boundary layer edge. Because of the high exit Mach number, L_t is significantly smaller than L_d.

The final design is shown in cross-section in Fig. 5(B). The subsonic region and the initial conical expansion are similar to those of the Mach 4 nozzle however, most of the contoured wall is manufactured from glass-reinforced plastic and is attached to the steel section with an aluminium flange. Glass-reinforced plastic was used in an effort to keep the nozzle mass small and to enable easy manufacture of the contoured wall. Damage to the plastic surface caused by contact with the high temperature test gas does not appear to be a problem.

4 EXPERIMENTAL CALIBRATION

The performance of each nozzle was evaluated by measuring the Pitot pressure P_{pitot} at planes normal to the nozzle axis. Refer to reports [6] and [7] for the original data sets for

the $M = 4$ nozzle and $M = 8$ nozzle respectively.

Each Pitot probe was fitted with a PCB-112 piezo-electric pressure transducer which measured the stagnation pressure behind a detached shock that formed over the upstream face of the probe. Several probes were mounted in a rake and a number of shots of the shock tunnel were made at each nominal operating condition.

Figure 6 shows the unfiltered histories of both nozzle supply pressure and Pitot pressure. These shots were typical of the shots that were made for the two calibration surveys. Note that the time origin is arbitrary as the recording device was triggered from the supply pressure signal and had an arbitrary pretrigger delay. All of the traces in Fig. 6 show the impulsive start and subsequent decay as discussed in Section 2. The time delay from shock reflection to the initial rise in the Pitot trace is the time for the primary shock to propagate through the nozzle. The relatively slow initial rise of the Pitot trace for the $M = 8$ nozzle is due to the filling of the probe cavity.

Although the absolute pressures are changing during the test flow period, a quasi-steady estimate can be obtained by considering Pitot traces normalized by a *time-shifted* supply pressure trace

$$P_{norm} = P_{pitot}(t)/P_s(t - \Delta t) \quad , \tag{2}$$

where Δt is the nominal transit time of a fluid particle from the shock reflection region to the probe position. Before applying this normalization procedure, individual traces were filtered by taking a *moving average* over a $0.05ms$ window.

4.1 Mach 4 Nozzle Performance

Filtered Pitot pressure traces at $x \simeq 0.67m$ and a number of radial locations are shown in Fig. 7(a). The supply conditions are $H_s \simeq 8.8MJ/kg$ and $P_s \simeq 13MPa$. The lower Pitot pressures measured at $r = 55mm$ are produced by the expansion fan propagating from the trailing edge of the nozzle wall. The relatively flat normalized traces shown in Fig. 7(b) indicate that the nozzle starts quickly and produces a long duration quasi-steady flow. The extreme values in the early part of the traces ($t < 2.6ms$) are a mixture of starting pulse and numerical artifact as the nominal time used in equation (2) is less than the time taken for the starting shock structure to traverse the nozzle.

Figure 8 shows the pitot profiles for a nominal supply pressure $P_s \simeq 13MPa$ and supply enthalpies $H_s \simeq 16MJ/kg$, $8.8MJ/kg$, and $6.6MJ/kg$. These representative values were obtained by taking an average of the filtered trace over a $0.5ms$ test period starting shortly after the passage of the starting shocks. The bar on each data point indicates the standard

deviation of the normalized trace during the same test period. The test flow core appears to extend to $r \simeq 40mm$ with a variation of $\pm 5\%$ in quasi-steady Pitot pressure. Profiles measured $0.1m$ further downstream [6] provided evidence that the flow divergence was less than 2.5 degrees but the shot-to-shot variation of the supply pressure measurements prevented an accurate determination.

4.2 Mach 8 Nozzle Performance

Filtered Pitot pressure traces at a number of radial locations are shown in Fig. 9(a). Here, the time base has been shifted such that the shock reflection occurred at $t = 0$. Note that, after reaching peak values, the traces near the nozzle axis show a rapid decay down to the levels of the outer traces. Note also the fall-off in average pressure and the decline in quality for the trace at $r = 142mm$. This location appears to be within the boundary layer formed along the nozzle wall.

Normalized Pitot pressure histories for shot 1406 are shown in Fig. 9(b) where $\Delta t = 0.50ms$. The trace at $r = 112mm$ illustrates the *classical* starting process in which the shock structure appears first followed by the unsteady expansion fan (the dip at $t = 0.6ms$ and subsequent rise to $t = 1.0ms$) and then steady conditions ($t > 1.2ms$). Toward the nozzle axis, the flow establishment is qualitatively different. Starting with the passage of the unsteady expansion ($t \simeq 0.75ms$), there is a large disturbance in the flow which is evident out to a radius $r = 90mm$. Such behaviour was obvious in most (but not all shots) and tended to be less significant at the highest enthalpy condition ($H_s \simeq 16MJ/kg$). For $H_s \geq 10MJ/kg$, the disturbed flow consumed a significant fraction of the available test time.

Figure 10 shows the timing of the events at the exit plane of the nozzle for shots with a nominal supply pressure $P_s \simeq 50MPa$. Estimates for the arrival time of the primary shock (line A) and the time to settle within 10% of steady state (line B) were computed using the quasi-one-dimensional model and the code described in [11]. The initial pressure within the nozzle was set to $P_{init} = 33Pa$ which is typical of conditions used in the T4 facility. Unfortunately precise values of P_{init} were not recorded. Approximate times for arrival of contaminated gas were taken from [1] and adjusted for the length of this nozzle.

The arrival time of the incident shock was well approximated by the quasi-one-dimensional model except at the $H_s \simeq 6.6MJ/kg$ condition. Here, either transient supply conditions or higher initial pressures in the test section may account for the differences. The settling time estimates (line B, Fig. 10) were relatively insensitive to either of these influences. In the experimental traces, the passage of the upstream head of the expansion fan was identified

as the point (after the shock structure passes) where the normalized Pitot pressure rose to the steady level. (Note that the trace may have exceeded the steady-state value after this time.) These times agree qualitatively with the predictions of the settling times (line B) but were all consistently delayed. This may be a multidimensional effect associated with the distortion of the upstream-facing shock and the unsteady expansion [11].

The experimental settling time seemed to occur approximately $0.3ms$ after the passage of the unsteady expansion. At the highest enthalpy ($H_s \simeq 16MJ/kg$) this settling time coincided with the estimated arrival time of the driver gas contamination however, the contamination time estimates were considered conservative and the flow disturbances were relatively small at this condition. Hence, some useful (albeit short) test time was expected to be available.

Once a test time was identified (by starting after the initial flow perturbations and then terminating before the expected time of contamination), a quasi-steady value was computed as the mean value of the filtered and normalized trace over the test period. These mean values, together with standard deviations computed over the same period, are shown in Fig. 11. The profiles are grouped with increasing supply enthalpy to the right and increasing supply pressure to the top. Other than some spurious data points near the nozzle axis, the profiles appear to be satisfactory (for shock tunnel work). If the nozzle contour was not performing well then, disturbances would be expected to focus near the nozzle axis. The stray data points may indicate the existence of such problems.

Computed distributions of Pitot pressure are compared with quasi-steady experimental values in Fig. 12. The supply conditions are $H_s \simeq 10MJ/kg$ and $P_s \simeq 50MPa$. Computed profiles for both viscous and inviscid wall boundary conditions are shown. Details of the full Navier-Stokes simulation are available in [11]. At $x = 1.8m$ the computed values for the viscous wall simulation fortuitously capture the spurious data points at the nozzle axis. Although the bulk of the computed values are reliable and match the experimental values well, those near the nozzle axis are subject to a particularly noisy boundary condition and should not be trusted. At $x = 2.0m$ there is obvious disagreement with the experiment near the axis. The experimental results also indicate that the physical boundary layer is thicker than that computed in the viscous-wall simulation. Note that the viscous-wall simulation was for laminar flow only whereas the physical flow may have been partly turbulent.

5 CONCLUDING REMARKS

The design of Mach 4 and a Mach 8 nozzles for use on a reflected shock tunnel has been described. The procedure treats the expanding flow in the nozzle as two conceptually separate flows. The initial conical expansion is treated as a quasi-one-dimensional expansion of a chemically-reacting gas. At the end of this conical expansion, the flow is assumed to be a source flow of a calorically perfect gas and the subsequent contoured section of the nozzle is determined by a method-of-characteristics analysis.

From the experimental point of view, the nozzles appear to produce a satisfactory test flows once a (quasi-)steady state is reached. Hence, the simple inviscid design approach is adequate but would benefit from the addition of a boundary layer correction for the Mach 8 nozzle. It may be possible to partially compensate for this oversight by manufacturing nozzle throats with smaller diameters while maintaining the current dimensions of the contoured expansion.

Although the steady performance of the Mach 8 nozzle is adequate, the settling times are much longer than predicted by the *classical* quasi-one-dimensional models. This delay in flow establishment is especially important at high enthalpy ($H_s > 16MJ/kg$) operating conditions as the nozzle supply conditions are maintained for relatively short times after shock reflection. Fortunately, this problem is compensated by the magnitude of the disturbances becoming small at higher H_s.

Acknowledgments

The design, fabrication and calibration of the nozzle were done at the University of Queensland. Dennis Susmilch fabricated the Mach 4 nozzle while Peter Killen and Ken Dudson fabricated the Mach 8 nozzle. Financial support was provided by the Australian Research Council and NASA[2]. Subsequent data reduction was done at ICASE, NASA Langley Research Center[3]. PJ also wishes to thank Richard Morgan and John Korte for helpful suggestions.

[2]grant NAGW-674
[3]contract NAS1-18605

References

[1] R. J. Stalker. Hypervelocity aerodynamics with chemical nonequilibrium. *Annual Review of Fluid Mechanics*, 21:37–60, 1989.

[2] H. G. Hornung. 28th Lanchester Memorial Lecture - experimental real-gas hypersonics. *Aeronautical Journal*, December, 1988.

[3] P. A. Jacobs, R. C. Rogers, E. H. Weidner, and R. D. Bittner. Flow establishment in a generic scramjet combustor. AIAA Paper 90-2096, 1990.

[4] W. R. Davies and L. Bernstein. Heat transfer and transition to turbulence in the shock-induced boundary layer on a semi-infinite flat plate. *Journal of Fluid Mechanics*, 36(1):87–112, 1969.

[5] R. G. Morgan, A. Paull, R. J. Stalker, P. A. Jacobs, N. Morris, I. Stringer, and C. Brescianini. Shock tunnel studies of scramjet phenomena. NASA Contractor Report 181721, 1988.

[6] P. A. Jacobs. A Mach 4 nozzle for hypervelocity flow. Department of Mechanical Engineering Report 9/89, University of Queensland, 1989.

[7] P. A. Jacobs. A Mach 8 nozzle for the T4 shock tunnel. Department of Mechanical Engineering Report 12/89, University of Queensland, 1989.

[8] P. A. Jacobs and R. J. Stalker. Design of axisymmetric nozzles for reflected shock tunnels. Department of Mechanical Engineering Report 1/89, University of Queensland, 1989.

[9] H. W. Liepmann and A. Roshko. *Elements of Gasdynamics*. John Wiley and Sons, New York, 1957.

[10] J. D. Anderson. *Modern Compressible Flow: with Historical Perspective*. McGraw-Hill, New York, 1982.

[11] P. A. Jacobs. Transient, hypervelocity flow in an axisymmetric nozzle. AIAA Paper 91-0295, 1991.

[12] H. O. Amann. Experimental study of the starting process in a reflection nozzle. *The Physics of Fluids Supplement I*, pages I–150 – I–153, 1969.

[13] C. E. Smith. The starting process in a hypersonic nozzle. *Journal of Fluid Mechanics*, 24:625–640, 1966.

[14] V. L. Gregorenko, A. M. Naumov, and N. I. Hvostor. Influence of nonstationary flow effects on test time of a hypersonic shock tunnel. *Scientific Notes of the Central Hydrodynamic Institute*, 15(5), 1984.

[15] A. B. Britan and E. I. Vasil'ev. Pecularities of the formation of the flow in a shaped shock-tube nozzle. *Soviet Physics Doklady*, 30(3):199–201, 1985.

[16] K. Hannemann. Design of an axisymmetric, contoured nozzle for the HEG. Technical Report DLR-FB90-04, DLR, 1990.

[17] N. R. Mudford, R. J. Stalker, and I. Shields. Hypersonic nozzles for high enthalpy nonequilibrium flow. *Aeronautical Quarterly*, May:113–131, 1980.

[18] D. Zonars. Nonequilibrium regime of airflows in contoured nozzles: theory and experiment. *A.I.A.A. Journal*, 4(1):57–63, 1967.

[19] J. A. Lordi, R. E. Mates, and J. R. Moselle. Computer program for the numerical solution of nonequilibrium expansions of reacting gas mixtures. NASA Contractor Report 472, 1966.

[20] P. A. Jacobs and C. M. Gourlay. An interactive method-of-characteristics program for gas-dynamic calculations. *International Journal of Engineering Education*, Accepted for Publication, 1990.

[21] G. E. Forsythe, M. A. Malcolm, and C. B. Moler. *Computer methods for Mathematical Computations.* Prentice-Hall, Englewood Cliffs, N. J., 1977.

[22] J. Lukasiewicz. *Experimental Methods of Hypersonics.* Marcel Dekker, New York, 1973.

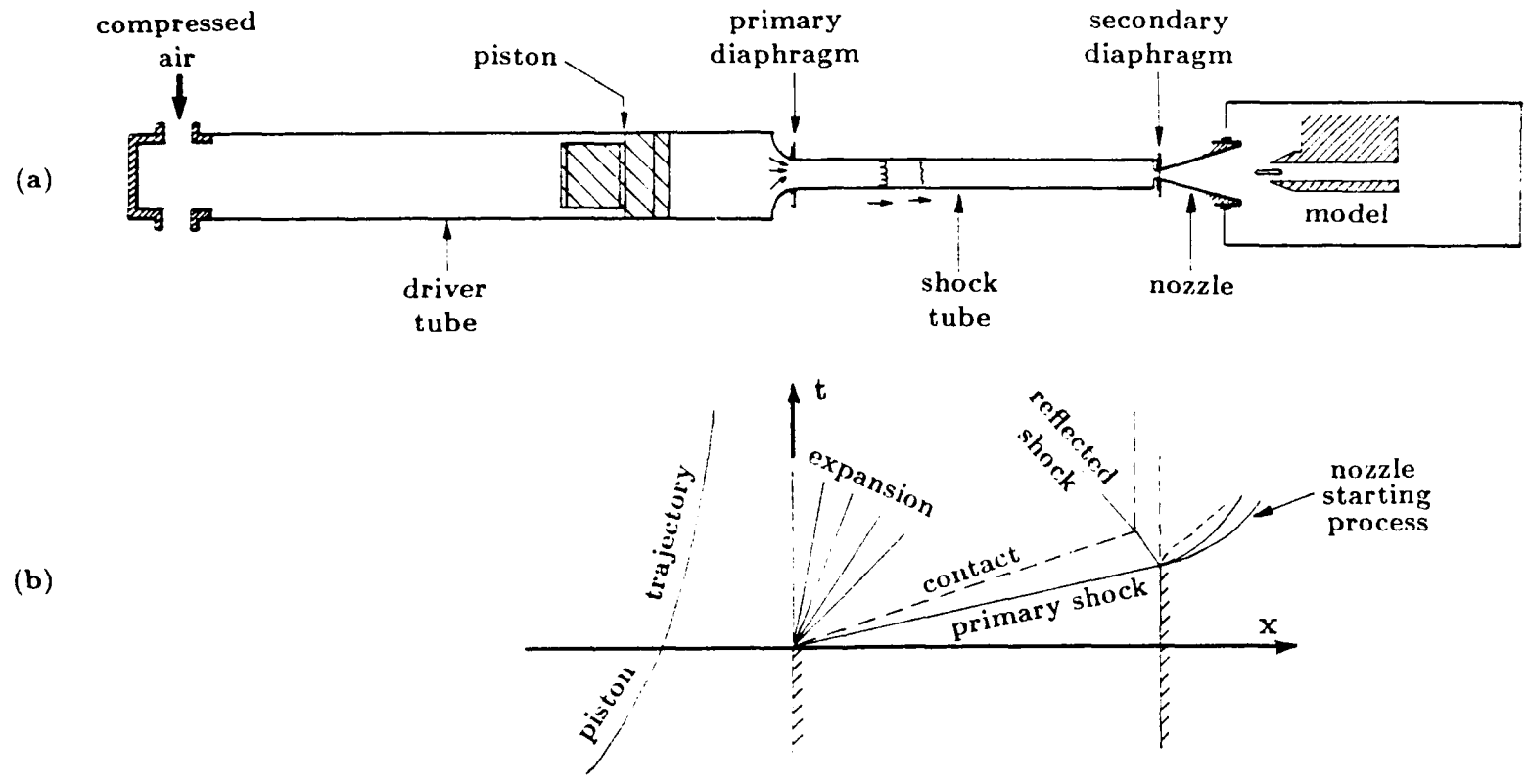

Figure 1: Reflected-shock tunnel operation. (a) Tunnel schematic, (b) $x - t$ wave diagram.

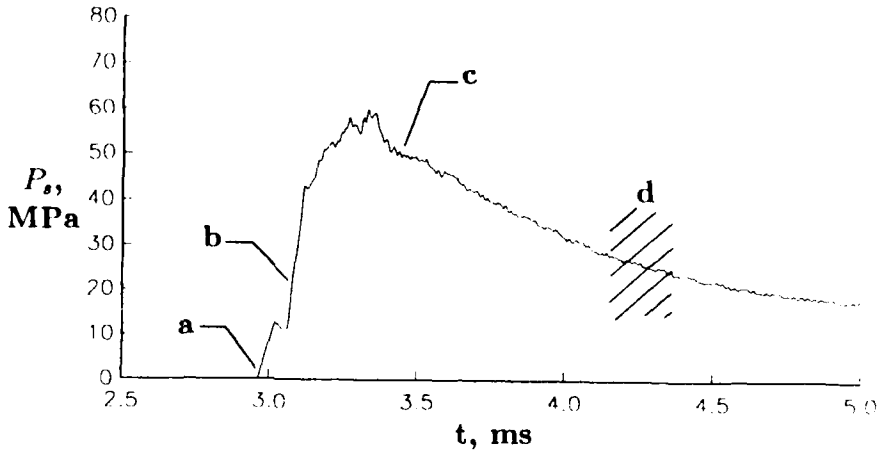

Figure 2: Typical history of the (unfiltered) nozzle supply pressure showing the principal events: (a) arrival of the incident shock; (b) reflected shock; (c) establishment of equilibrium pressure; (d) driver gas contamination.

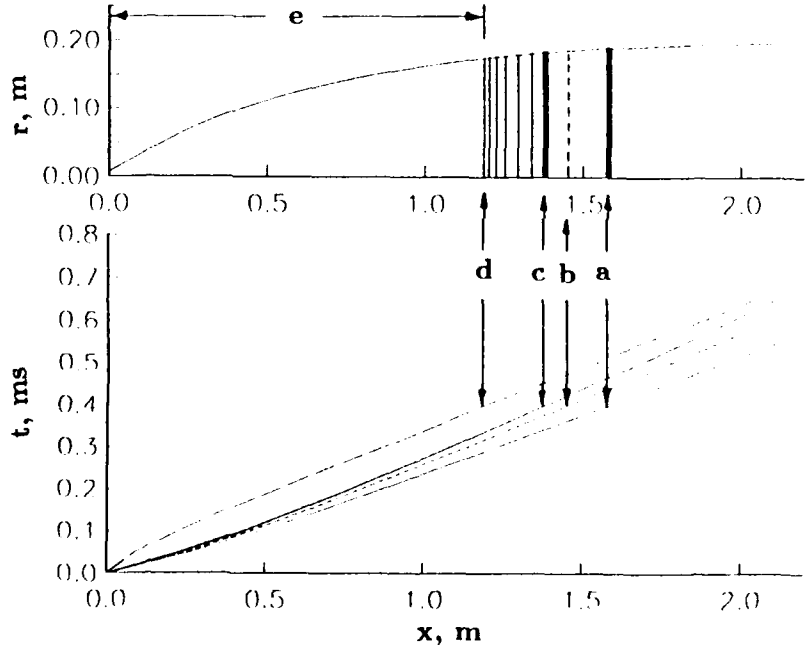

Figure 3: Quasi-one-dimensional model of the nozzle starting process in both the physical plane and the $x - t$ plane. Labelled features are: (a) primary shock; (b) contact surface; (c) upstream-facing shock; (d) upstream head of the unsteady expansion; (e) steady expansion.

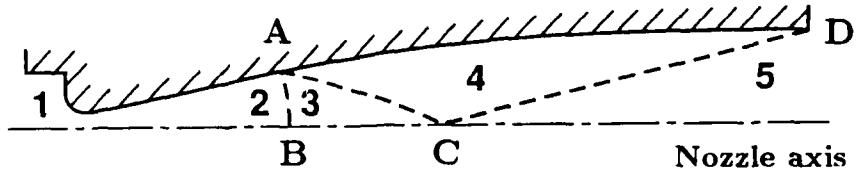

Figure 4: Schematic view of a contoured nozzle showing regions of: (1) stagnant nozzle supply gas; (2) transition to source flow; (3) source flow; (4) transition to parallel flow; (5) parallel flow.

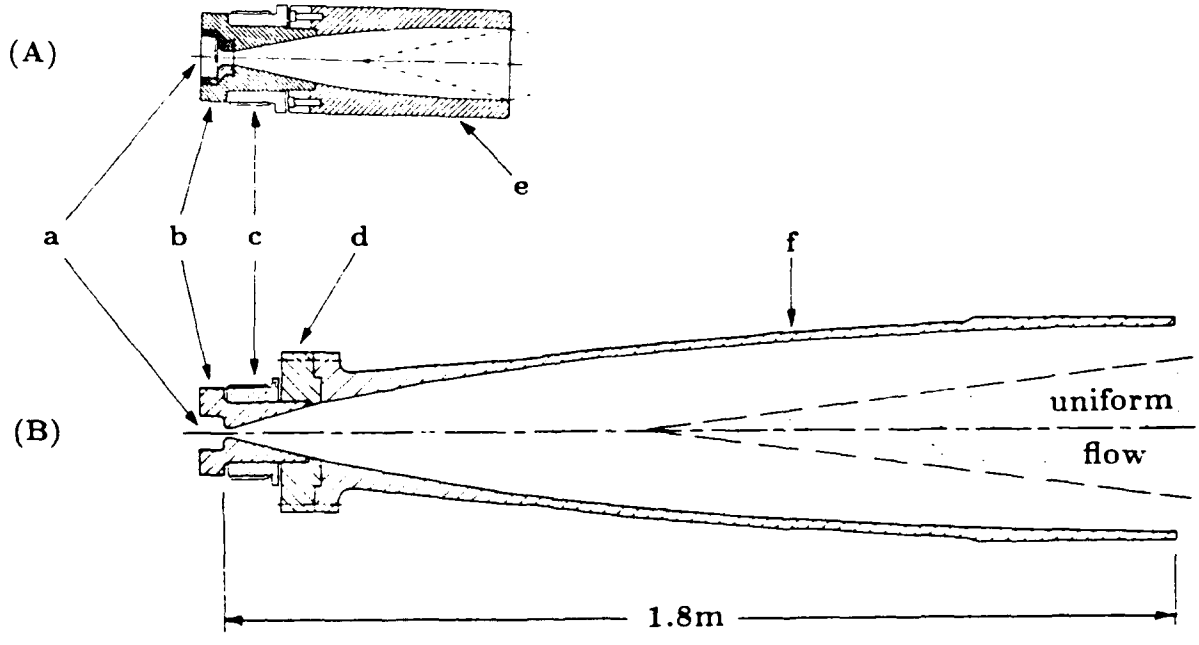

Figure 5: Sectional view of the (A) Mach 4 and (B) Mach 8 nozzles showing (a) shock-reflection/ nozzle-supply region; (b) high-tensile steel section; (c) retaining nut; (d) aluminium flange ($M = 8$); (e) aluminium contoured section ($M = 4$); (f) glass-reinforced plastic section ($M = 8$).

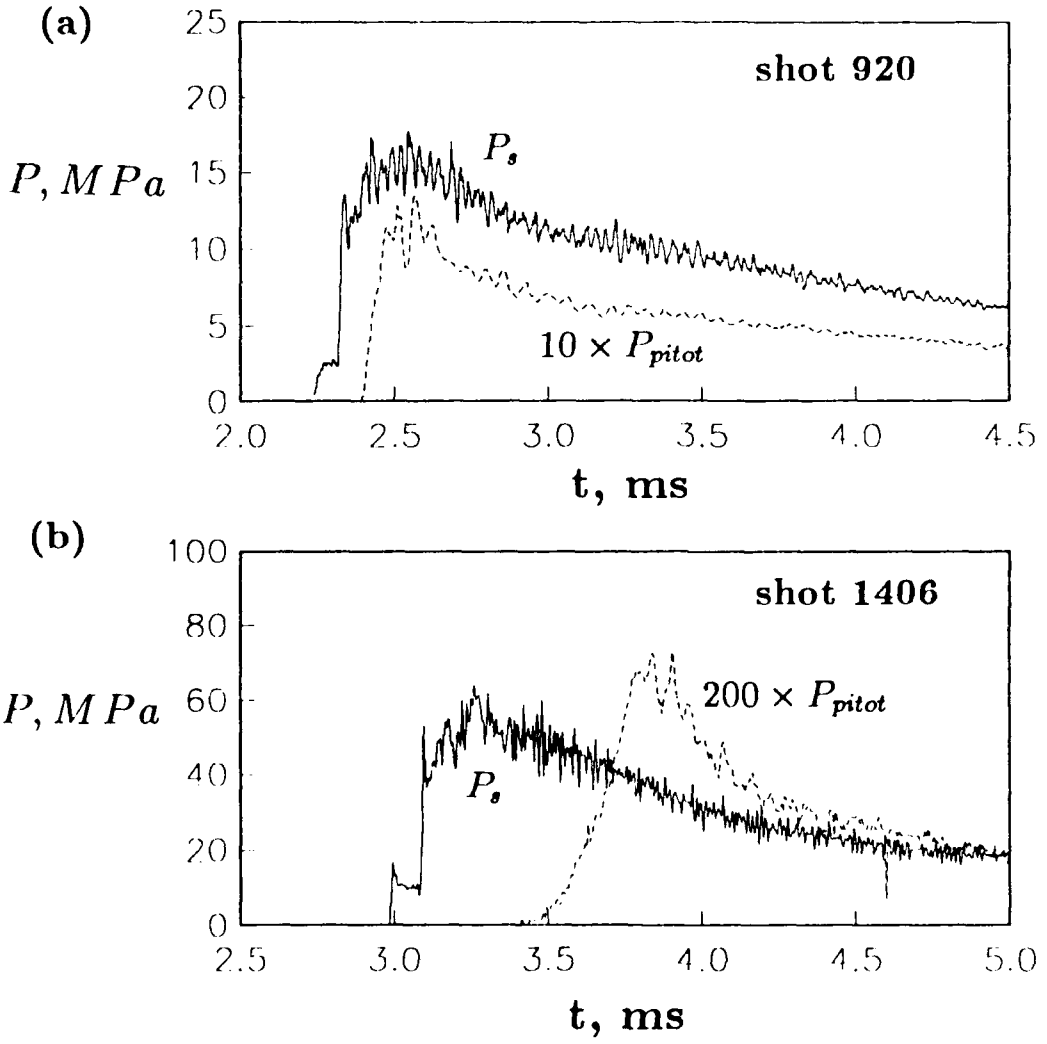

Figure 6: Typical histories for the nozzle supply pressure (solid line) and the Pitot pressure (dashed line): (a) $M = 4$ nozzle, $x \simeq 0.67m$, $r \simeq 0$, $P_{rupture} = 28.3MPa$, $\lambda = 77$; (b) $M = 8$ nozzle , $x \simeq 1.8m$, $r \simeq 0$, $P_{rupture} = 56.6MPa, \lambda = 60$. These traces are unfiltered.

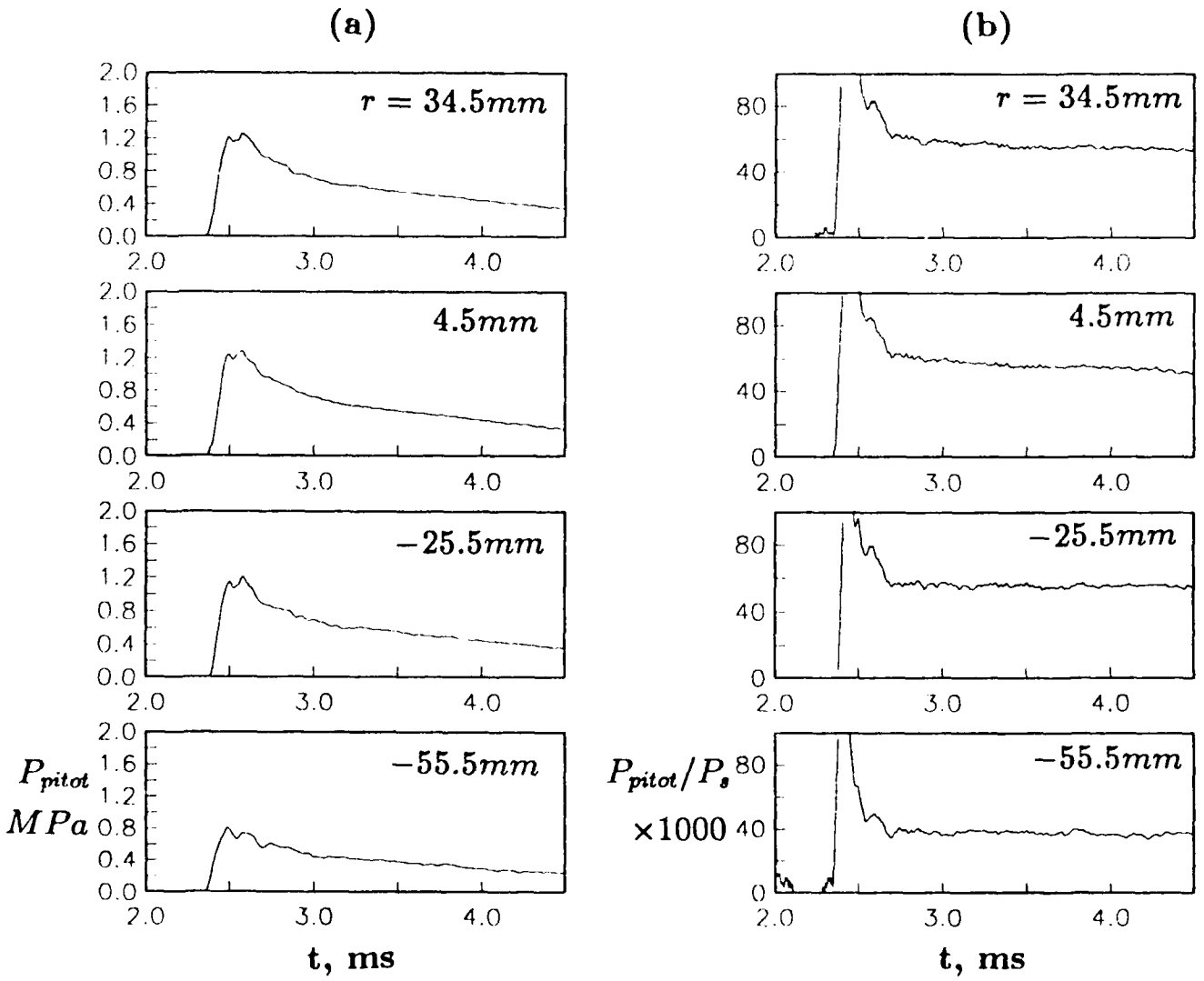

Figure 7: (a) Filtered and (b) Normalized Pitot pressure histories at $x \simeq 0.67m$ for shot 920 ($M = 4$).

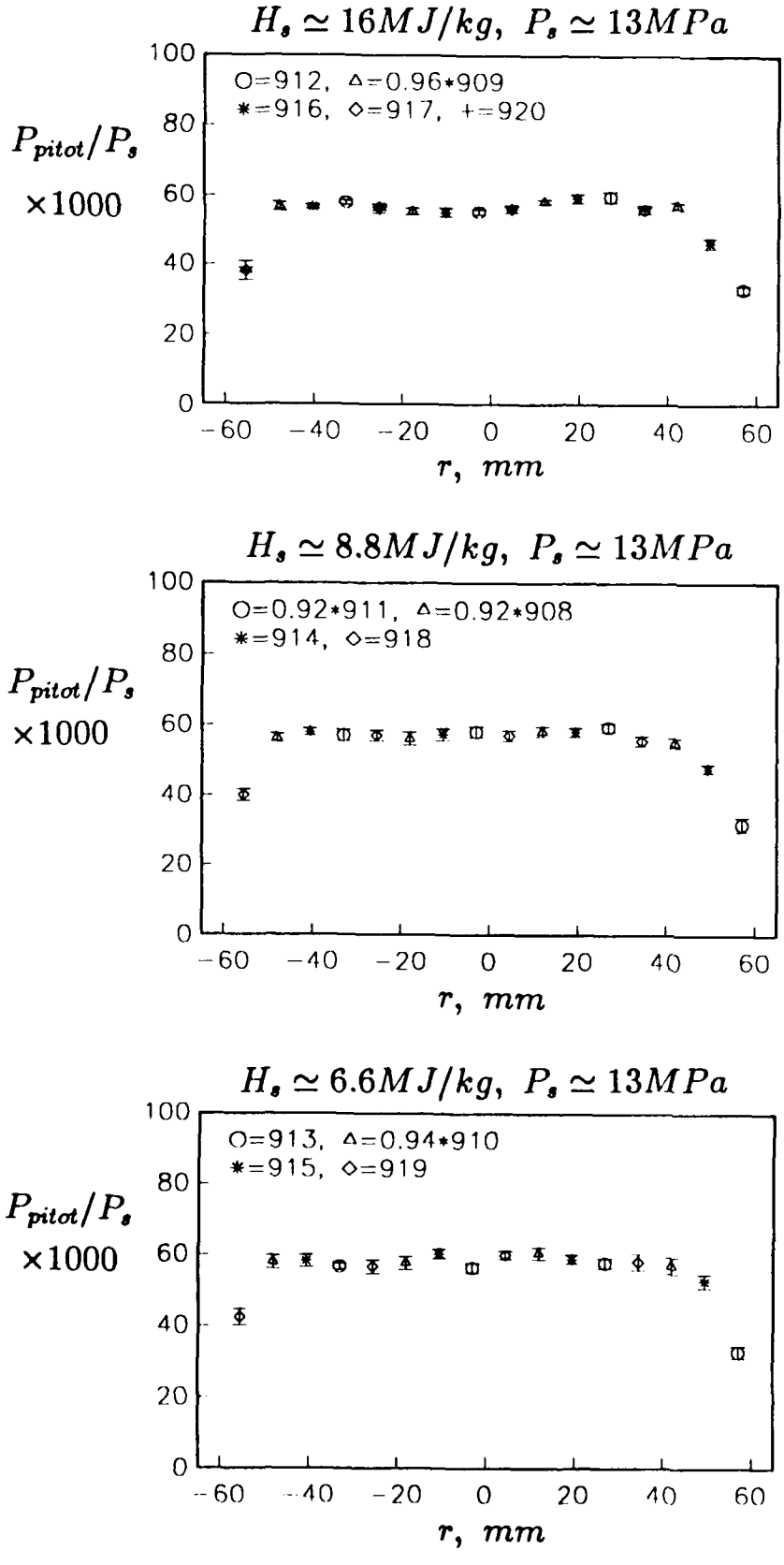

Figure 8: Quasi-steady Pitot pressure profiles for the $M = 4$ nozzle at $x \simeq 0.67m$.

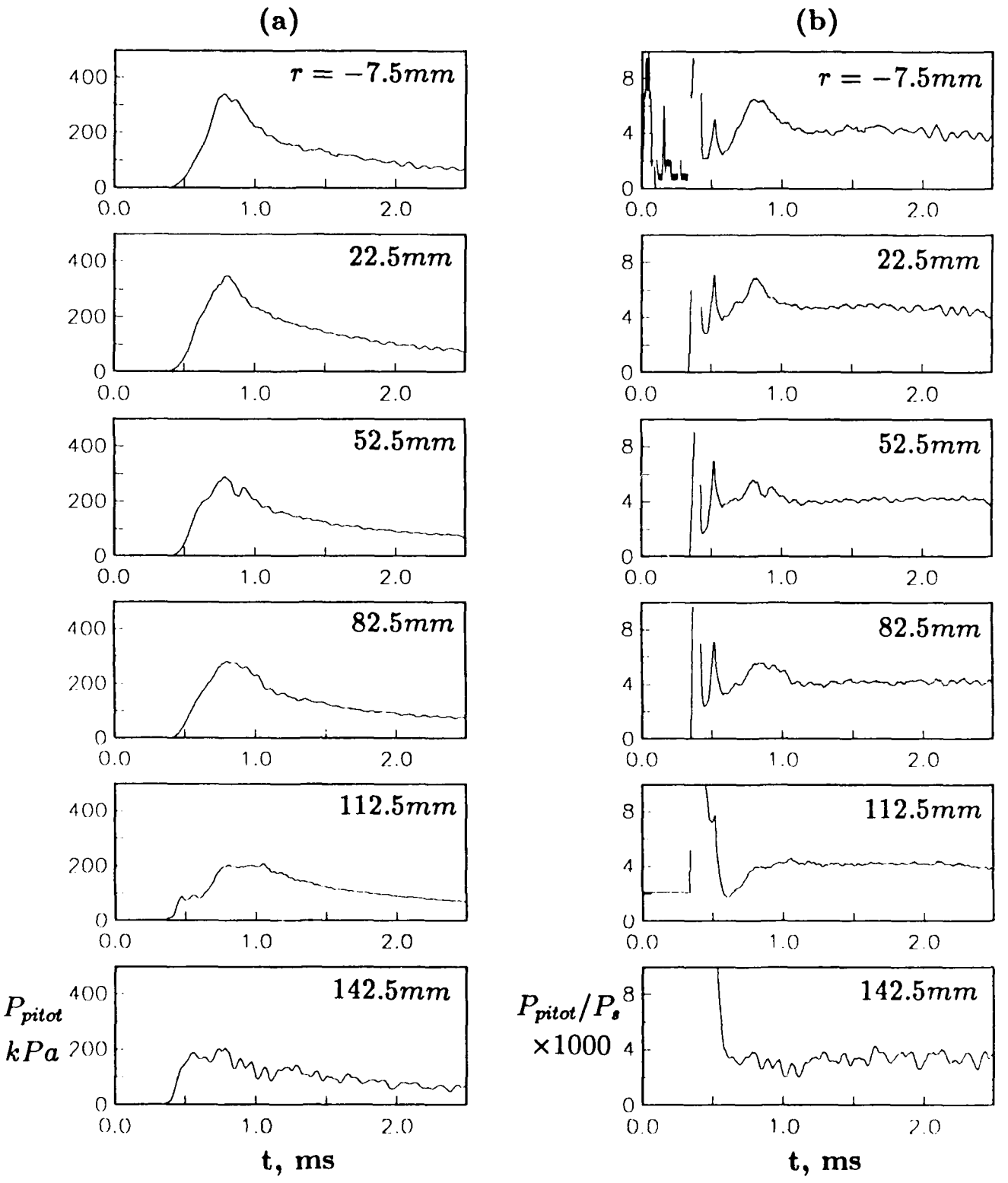

Figure 9: (a) Filtered and (b) Normalized Pitot pressure histories at $x \simeq 1.8m$ for shot 1406 ($M = 8$). Note that the time base has been shifted such that shock reflection occurs at $t = 0$.

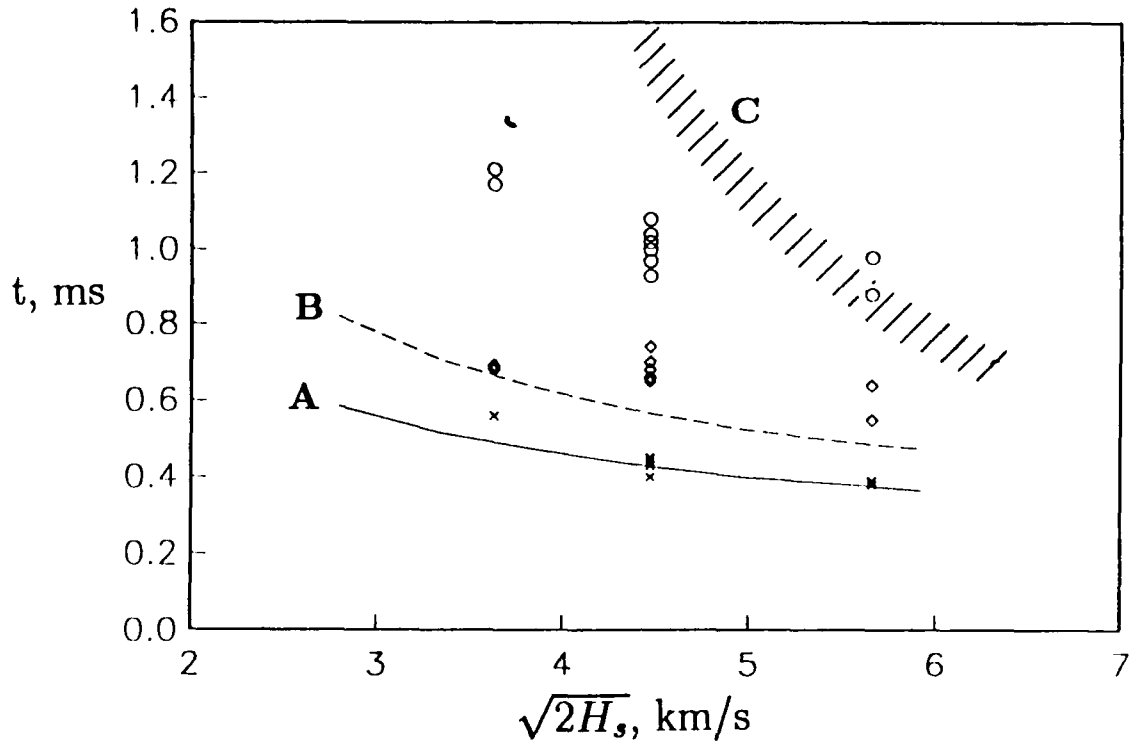

Figure 10: Times at which events occur at the $M = 8$ nozzle exit plane. A. primary shock arrival (Q1D model); B. settling time (10%, Q1D model); C. contamination by driver gas; $\times$ primary shock arrival (experimental); $\bigcirc$ settling time (experimental); $\diamond$ passage of the expansion fan (experimental).

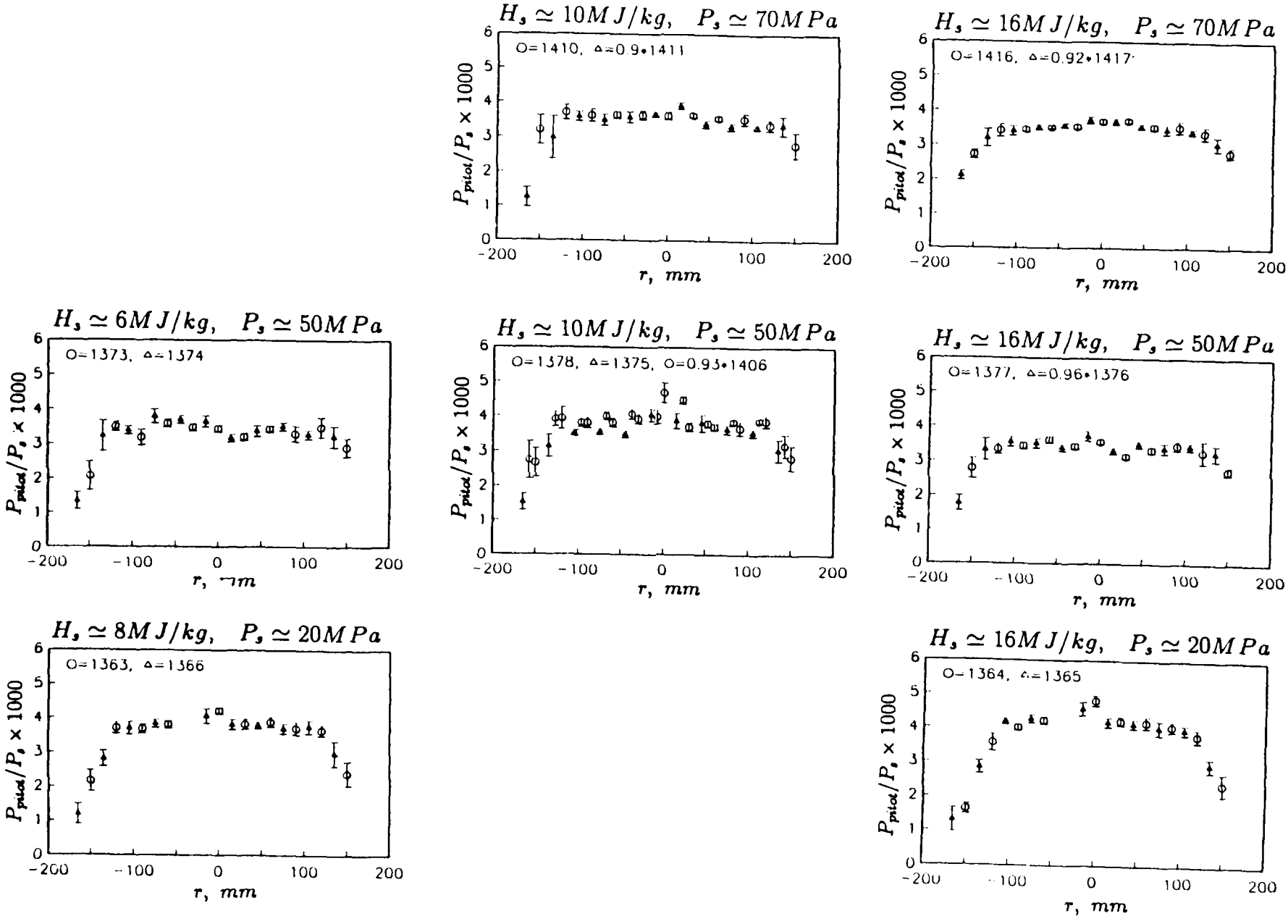

Figure 11: Quasi-steady Pitot pressure profiles for the $M = 8$ nozzle at $x \simeq 1.8m$.

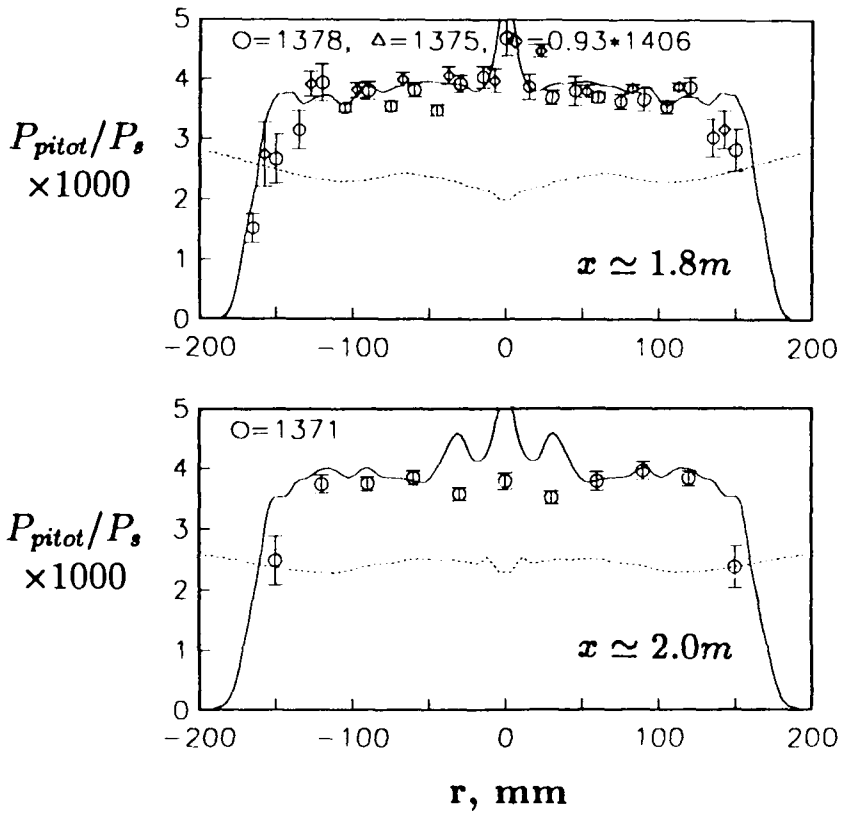

Figure 12: Quasi-steady normalized Pitot pressures across the $M = 8$ nozzle exit plane ($x \simeq 1.8m$) and further downstream at $x \simeq 2.0m$: solid line = viscous-wall simulation; dash = inviscid-wall simulation.

NASA National Aeronautics and Space Administration

Report Documentation Page

1. Report No.	2. Government Accession No.	3. Recipient's Catalog No.
NASA CR-187533 ICASE Report No. 91-24		

4. Title and Subtitle	5. Report Date
MACH 4 AND MACH 8 AXISYMMETRIC NOZZLES FOR A SHOCK TUNNEL	February 1991
	6. Performing Organization Code

7. Author(s)	8. Performing Organization Report No.
P. A. Jacobs R. J. Stalker	91-24
	10. Work Unit No.
	505-90-52-01

9. Performing Organization Name and Address	11. Contract or Grant No.
Institute for Computer Applications in Science and Engineering Mail Stop 132C, NASA Langley Research Center Hampton, VA 23665-5225	
	13. Type of Report and Period Covered
12. Sponsoring Agency Name and Address	Contractor Report
National Aeronautics and Space Administration Langley Research Center Hampton, VA 23665-5225	14. Sponsoring Agency Code

15. Supplementary Notes

Langley Technical Monitor:
Michael F. Card

To be Submitted to The Aeronautical Journal

Final Report

16. Abstract

This study examines the performance of two axisymmetric nozzles which were designed to produce uniform, parallel flow with nominal Mach numbers 4 and 8. A free-piston-driven shock tube was used to supply the nozzle with high-temperature, high-pressure test gas. The inviscid design procedure treated the nozzle expansion in two stages. Close to the nozzle throat, the nozzle wall was specified as conical and the gas flow was treated as a quasi-one-dimensional chemically-reacting flow. At the end of the conical expansion, the gas was assumed to be calorically perfect and a contoured wall was designed (using Method-of-Characteristics) to convert the source flow into a uniform and parallel flow at the end of the nozzle. Performance was assessed by measuring Pitot pressures across the exit plane of the nozzles and, over the range of operating conditions examined, the nozzles produced satisfactory test flows. However, there were flow disturbances in the Mach 8 nozzle flow that persisted for significant times after flow initiation.

17. Key Words (Suggested by Author(s))	18. Distribution Statement
axisymmetric nozzle; shock tunnel	09 - Research and Support Facilities (Air) 34 - Fluid Mechanics and Heat Transfer Unclassified - Unlimited

19. Security Classif. (of this report)	20. Security Classif. (of this page)	21. No. of pages	22. Price
Unclassified	Unclassified	26	A03

NASA FORM 1626 OCT 86